

Efficient simulation of inhomogeneously correlated systems using block interaction product states

Yifan Cheng,¹ Zhaoxuan Xie,² Xiaoyu Xie,^{3,*} and Haibo Ma^{3,†}

¹*School of Chemistry and Chemical Engineering, Nanjing University, Nanjing 210023, China*

²*Department of Physics and Arnold Sommerfeld Center for Theoretical Physics (ASC), Ludwig-Maximilians-Universität München, Theresienstr. 37, München D-80333, Germany*

³*Qingdao Institute for Theoretical and Computational Sciences, School of Chemistry and Chemical Engineering, Shandong University, Qingdao 266237, China*

(Dated: August 16, 2024)

The strength of DMRG lies in its treatment of identical sites that are energetically degenerate and spatially similar. However, this becomes a drawback when applied to quantum chemistry calculations for large systems, as entangled orbitals often span broad ranges in energy and space, with notably inhomogeneous interactions. In this study, we propose addressing strong intra-fragment and weak inter-fragment correlations separately using a multi-configuration block interaction product state (BIPS) framework. The strong correlation is captured in electronic states on fragments, considering entanglement between fragments and their environments. This method has been tested in various chemical systems and shows high accuracy and efficiency in addressing inhomogeneous effects in quantum chemistry.

INTRODUCTION

Thanks to the high compression of the matrix product state (MPS) representation of the wave function and the efficient site-by-site iterative sweeping optimization algorithm, the density matrix renormalization group (DMRG) [1–6] method has been established as a powerful computational tool in accurately simulating one-dimensional (1D) strongly correlated systems. DMRG is remarkably efficient when applied to 1D chains with only local interactions and nearly identical sites, as typically encountered in physical models such as the Heisenberg [7, 8] or Hubbard [9, 10] Hamiltonian.

However, in the realm of quantum chemistry, large and realistic correlated systems often exhibit inhomogeneous electron correlations. For instance, within conjugated polymers, the correlation within a single monomer fragment is typically more pronounced than the inter-fragment correlation between different monomer fragments. Because *ab initio* quantum chemistry Hamiltonian encompasses numerous long-range interactions and four-operator terms, quantum chemistry DMRG (QC-DMRG) calculations [11–14] scale steeply ($O(k^4m^2) + O(k^3m^3)$) with system size (k , the number of active orbitals) and necessitate a substantial number ($m \sim 10^{3–4}$) of truncated renormalized bases, also known as auxiliary bond dimensions. Given their vast size, many chemical systems with inhomogeneous correlations, such as polymers, molecular aggregates, and polynuclear transition metal complexes, are far beyond the current capability of QC-DMRG. Hence, there is a pressing need for developing novel efficient methods tailored to these inhomogeneously correlated systems.

To address these challenges, specialized tensor networks (TNs) like the comb tensor network (CTN) [15] have been proposed, which assign sites with different en-

tangling environments to distinct node levels. While the CTN approach effectively represents correlations of varying strengths, its computational cost scales as the fourth power of the bond dimension (m^4), and constructing the quantum chemistry Hamiltonian as a tensor network operator (TNO) is highly non-trivial. Consequently, its application to quantum chemical systems remains limited.

Alternative approaches focus on coarse-graining idea, which groups the neighboring strongly correlated sites into single coarse grained large site, sometimes called as "cluster", to pre-package strong intra-fragment correlation and simplify the simulation of the whole system. Methods like the cluster mean field (cMF) [16] or localized active space self-consistent field (LASSCF) [17] describe the intra-fragment correlation at the exact diagonalization (ED) level while treating weaker inter-fragment correlations with mean-field theory. The cluster DMRG (cDMRG) [1, 18] method builds on this and uses a small bond dimension to sweep over the coarse-grained large sites to further describe the inter-fragment correlation that is neglected in mean field treatment. However, these methods still face time-consuming challenges due to the large local Hilbert spaces that arise in coarse-grained sites. There are some attempts to keep only few energetically low-lying adiabatic states to reduce the local Hilbert space, such as real-space renormalization group (RSRG) [19], and contractor renormalization group (CORE) [20] methods. However, the local adiabatic states derived from an isolated fragment's calculation cannot adequately represent the realistic inter-fragment interactions, just like the well-known breakdown of numerical renormalization group (NRG) for correlated systems [21].

In this letter, we introduce a novel coarse-grained method designed to simulate inhomogeneously correlated systems efficiently. This approach independently ad-

dressess the strong intra-fragment correlations and the weak inter-fragment correlations, employing a block interaction product state (BIPS) [22] formulation. For each fragment, a compact set of renormalized local states is optimally constructed, taking into account the environmental effect. This is achieved by performing a many-body correlated-level calculation on a model system that comprises the local physical system and its associated auxiliary bath space. When seamlessly integrated with cDMRG, this method offers an accurate and computationally efficient way to describe inhomogeneously correlated systems.

MPS BASICS

Considering a system composed of k sites, each of which have d local states. The wave function can be expressed as an MPS structure with different canonical form considering the gauge freedom of TNs. Assuming the orthogonality center site p divide the chain into left system and right environment blocks, then the wave function can be written in the mixed canonical form as:

$$\begin{aligned} |\Psi\rangle &= \sum_{\{\sigma_i\}} \sum_{\{a_i=1\}}^{\{m_i\}} U_{1,a_1}^{\sigma_1} \cdots M_{a_{p-1},a_p}^{\sigma_p} \cdots V_{k-1,1}^{\sigma_k*} |\sigma_1 \cdots \sigma_p \cdots \sigma_k\rangle \\ &= \sum_{\sigma_p} \sum_{a_{p-1},a_p} (M_{a_{p-1},a_p}^{\sigma_p} |L_{a_{p-1}}\rangle \otimes |\sigma_p\rangle) \otimes |R_{a_p}\rangle \\ &= \sum_{a_p=1}^{m_p} S_{a_p} |L_{a_p}\rangle \otimes |R_{a_p}\rangle, \end{aligned} \quad (1)$$

in which $U/V/M_{a_{i-1},a_i}^{\sigma_i}$ represents an element of the local rank-3 tensor, and $\{|L_{a_p}\rangle\}$ and $\{|R_{a_p}\rangle\}$ denote renormalized states of system and environment blocks, respectively. Since $\{|L_{a_p}\rangle\}$ are eigenvectors of the reduced density matrix (RDM) for system block, meaning that the RDM is diagonal when represented in such bases:

$$\rho_{sys} = \text{Tr}_{env}(|\Psi\rangle\langle\Psi|) = \sum_{a_p=1}^{m_p} S_{a_p}^2 |L_{a_p}\rangle\langle L_{a_p}|. \quad (2)$$

Therefore, these renormalized states can be seemed as the most compact many-particle bases to represent the Hilbert space of system block, which is also the key ingredient behind the success of DMRG.

Although it is principally possible to simulate inhomogeneous correlation using DMRG with a variable bond dimension—for example, by using dynamical block state selection (DBSS)[23] to determine auxiliary states based on singular values—the efficient application of DMRG to chemical systems is still limited by high computational costs. The factors of k^4/k^3 in a long chain of sites and m^2/m^3 with large m values collectively lead to prohibitive computational expenses for large chemical systems.

BIPS

Considering the expensive computational cost of DMRG for large chemical systems, we suggest addressing the inhomogeneous electron correlation (the strong intra-fragment correlation and weak inter-fragment correlation) separately. By fusing the orbitals that belong to the same strongly correlated regions together, the overall wave function can be formulated as:

$$\begin{aligned} |\Psi\rangle &= \sum_{\alpha,\beta,\cdots,\omega} c_{\alpha_1,\beta_2,\cdots,\omega_N} |\alpha_1\beta_2\cdots\omega_N\rangle \\ &= \sum_{\alpha,\beta,\cdots,\omega} \sum_{\{\tilde{a}_I=1\}}^{\{\tilde{m}_I\}} M_{1,\tilde{a}_1}^{\alpha_1} M_{\tilde{a}_1,\tilde{a}_2}^{\beta_2} \cdots M_{\tilde{a}_{N-1},1}^{\omega_N} |\alpha_1\beta_2\cdots\omega_N\rangle. \end{aligned} \quad (3)$$

In this equation, N is the number of fused regions (blocks/clusters) in system and Greek letters label the states of particular region. The indices $\{\tilde{m}_I\}$, $\{\tilde{a}_I\}$ are utilized to be distinguished from $\{m_i\}$, $\{a_i\}$ in the standard MPS. In this form of wave function, the total Hilbert space is spanned by the product of electronic states from different regions, which are herein named block interaction product states (BIPSs). This generalized formula can yield the standard MPS form or the cMF wave function if the selected region is reduced or the local Hilbert space is limited. Principally, it holds true for any system when enough local bases are utilized, while we find only several appropriately selected states can already achieve chemical accuracy for numerous molecular systems of interest. These selected states encapsulate the strong correlation inside and result in a more dense representation of the local Hilbert space.

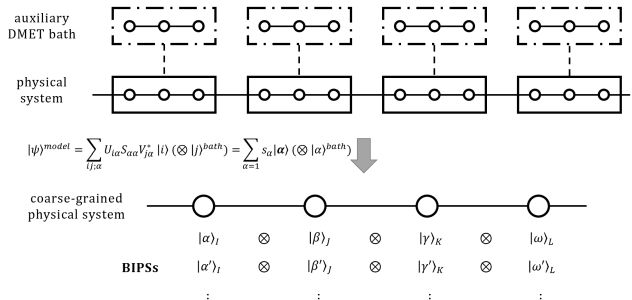


FIG. 1. Algorithms for constructing BIPS using the auxiliary DMET bath environment.

Our algorithm for obtaining BIPSs in quantum chemistry begins with localized and orthogonal molecular orbitals. By partitioning the system into N block fragments, these orbitals can be assigned to each block according to their dominant atomic orbital contributions. For each block fragment, a set of bath orbitals must be defined to simulate the environmental effect on the construction of local states. This set should be small to avoid

costly calculations of the model system, which includes the fragment of interest and its defined bath orbitals. In this case, we utilize one-shot density matrix embedding theory (DMET) [24] to generate a bath orbital space that has only the same size as the local orbital space for each individual fragment (as Fig 1 shows). To construct optimal local states, the model system should be treated at a high correlated level, such as DMRG, TN, or ED, in order to obtain $|\psi\rangle^{model}$. Subsequently, the fragment's RDM can be constructed from the model system's wave function by tracing out the bath degrees of freedom, and then diagonalized to obtain the renormalized local state bases for the fragment of interest with large eigenvalues. These renormalized local states provide an optimal set of bases for accurately describing the strong intra-fragment correlation under a weakly correlated environment.

BIPS-DMRG

Generally, the construction of local bases under the framework of MPS using DMRG is straightforward. However, one still need to obtain the BIPS coefficient $c_{\alpha_1, \beta_2, \dots, \omega_N}$. The standard configuration interaction (CI) is not suitable to solve for the coefficients because it requires calculating the Hamiltonian element between every pair of configurations and breaks the encapsulation of strong intra-fragment correlation. A more appropriate way is to maintain the structure of local states and precompute the operator quantities localized in each cluster. In other words, a cluster MPO with physical bonds, which represents the selected local states, should be constructed.

The construction procedure of cluster-MPO is similar to the propagation procedure in standard DMRG. When considering the non-Abelian spin-SU(2) symmetry, the tensors that appear during propagation will consist of reduced matrix elements. During tensor contraction, the coupling coefficients must be multiplied, and as a result, the formulation can be expressed as follows:

$$(W_{b_I, b_{I+i}}^{a_i^*, a_i})^{[k]} = \sum_{\substack{\sigma_i^*, \sigma_i, \\ a_{i-1}^*, a_{i-1}, \\ b_{I+i-1}}} \sqrt{(2S_{b_{I+i-1}} + 1)(2k + 1)} \times W(S_{b_I} k_1, S_{b_{I+i}} k_2; S_{b_{I+i-1}} k) \\ \times \begin{bmatrix} S_{a_{i-1}} & S_{\sigma_i} & S_{a_i} \\ k_1 & k_2 & k \\ S_{a_{i-1}^*} & S_{\sigma_i^*} & S_{a_i^*} \end{bmatrix} (W_{b_I, b_{I+i-1}}^{a_{i-1}^*, a_{i-1}})^{[k_1]} (U_{a_{i-1}, a_i}^{\sigma_i})^* (W_{b_{I+i-1}, b_{I+i}}^{\sigma_i^*, \sigma_i})^{[k_2]} U_{a_{i-1}, a_i}^{\sigma_i} \quad (4)$$

Here, $(W_{b_I, b_{I+i}}^{a_i^*, a_i})^{[k]}$ is an element of the i -th primitive MPO in block I , where $\{b_i\}$ labels the MPO's auxiliary bonds. The S_x represents the spin quantum number of index x , k denotes the spin quantum number of $(\hat{W})^{[k]}$ itself, $W(j'k_1, jk_2; j''k)$ is the Racah coefficient, and the bracketed term is the product of a Wigner-9j symbol and a normalization factor.

After obtaining the cluster-MPO, it can be directly integrated into any MPS-based DMRG program. A CI-like procedure (with selection) can also be easily executed since calculating the Hamiltonian between two BIPSs only requires the tensor contraction between the cluster-MPO and two cluster-MPSs with one auxiliary bond dimension. However, we believe that after the encapsulation of strong correlations, the remaining weaker but more homogeneous inter-fragment correlations should be more readily obtained by the DMRG procedure. The one-site DMRG algorithm with perturbative subspace expansion [25, 26] is typically preferred due to its lower computational cost compared to the two-site algorithm. Nonetheless, in BIPS-DMRG, where fragment states are

compressed and the bond dimension for weaker correlations is small ($\tilde{m} \sim 100 - 200$), the two-site DMRG can also be used for better convergence.

Unlike the comb TN, the cluster-MPO in BIPS-DMRG remains a 1D chain rather than a non-1D TN structure, reducing computational costs. The total computational cost of BIPS-DMRG originates from two parts: (1) standard DMRG within the model space ($O(N\tilde{k}^4m^2) + O(N\tilde{k}^3m^3)$) and (2) cDMRG for acquiring BIPSs' coefficients ($O(k^4\tilde{m}^2) + O(k^3\tilde{m}^3)$). Here, $\tilde{k} := k/N$ represents the number of sites within the model system. It is easy to observe the separation between large bond dimensions and a long chain of sites. As a result, the scenario where two factors collectively result in high computational costs in DMRG is mitigated by separating the inhomogeneous electron correlation in BIPS-DMRG.

This framework not only enables highly accurate energy calculations but also allows for the definition of several diabatic states (BIPSs). By using an efficient sampling algorithm [27], significant BIPSs can be identified, aiding in the analysis of the global wave function's physi-

cal meaning. Calculating Hamiltonian elements between these important BIPSSs can further reveal diagonal energies and coupling magnitudes, enabling the construction of a highly-compressed effective Hamiltonian.

NUMERICAL RESULTS

To assess the validity of BIPS-DMRG and demonstrate the inhomogeneous interactions in chemical systems, we applied the BIPS-DMRG method to several chemical systems, including both bonding and non-bonding interactions (Fig 2). The cMF calculation is first performed to achieve well-localized orbitals. Subsequent calculations, including DMRG, BIPS-DMRG, and cDMRG, are based on the optimized cMF orbitals. The preparation of cMF orbitals and DMET bath orbitals was performed using the PySCF [28] and MRH [29] packages. All other electronic structure calculations were implemented based on the Kylin software package [30].

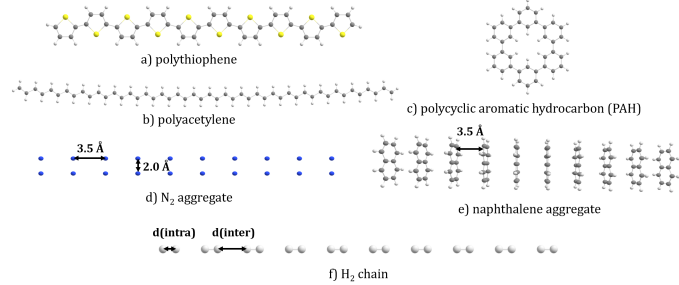


FIG. 2. Testbed systems for BIPS-DMRG explored in this work.

We compared the results of BIPS-DMRG with other methods (Tab I), including DMRG, cMF, and active space decomposition (ASD)-DMRG [31], which is cDMRG using the energetically low-lying eigenstates as local states. The number of preserved states within different quantum number sectors in ASD-DMRG is kept same as in BIPS-DMRG. It can be observed that, compared to HF, cMF can capture the majority of the electron correlation, which is intra-fragment correlation. However, the remaining inter-fragment correlation is not negligible, contributing approximately 5-100 mE_h. Although ASD-DMRG can improve over the results of cMF, it exhibits much lower efficiency in recovering inter-fragment correlations compared to BIPS-DMRG. This illustrates that the preserved local states, which consider environmental effects in BIPS-DMRG, are more advantageous than the isolated local states in ASD-DMRG. It was demonstrated that regardless of whether the system is non-bonding or bonding, BIPS-DMRG consistently yields satisfactory results (with errors within 1-3 mE_h). Note that weaker inter-fragment correlations not only result in fewer preserved states but also a smaller bond

dimension in BIPS-DMRG, and these two parameters should be comparable if targeting only a single electronic state. In this study, we choose to keep these two parameters the same to simplify discussion, i.e., $n_{\text{state}} \equiv \tilde{m}$.

Then we illustrate the efficiency of BIPS-DMRG method compared to standard QC-DMRG. We investigate the convergence of BIPS-DMRG with n_{state} and \tilde{m} in cluster DMRG using the polythiophene molecule (Fig 2.a). The energy error and speedup compared to DMRG results with $m = 1000$ are shown in Fig 3. The results indicate a dramatic decrease in energy error with an increase in the number of preserved states. When the number of preserved states reaches 128, the energy error is within 0.1 mE_h, while BIPS-DMRG maintains the speedup of more than 2.

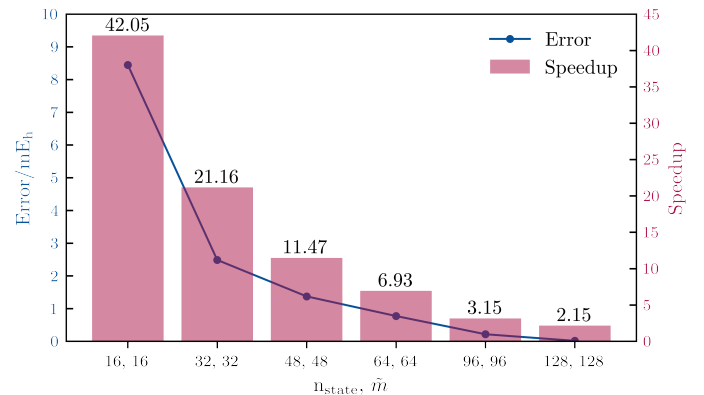


FIG. 3. The energy error and speedup of BIPS-DMRG with the number of preserved states (n_{state}) and the bond dimension (\tilde{m}).

The BIPS-DMRG method can be straightforwardly generalized to calculate multiple low-lying excited states simultaneously by diagonalizing the state-averaged reduced density matrix to define renormalized local bases. Table II presents results for the first six low-lying states of polythiophene, showing that the energy deviations are still less than 10 milli-Hartree, although the excited states exhibit slightly larger errors than the ground state. This is because defining appropriate bath orbitals for excited state calculations is non-trivial compared to those for the ground state. In this work, we did not explore the most suitable bath orbitals for excited state calculations, but rather showcased the capability of BIPS-DMRG in treating excited states as a prototype. The renormalized local state bases facilitate wave function analysis, revealing that the lowest excited states (S_1 - S_5) are primarily doubly excited (TT states). We selected 31 diabatic states with significant coefficients (> 0.1) and further constructed a compressed effective Hamiltonian matrix, as detailed in the Supporting Information.

In the end, we compared the accuracy of BIPS-DMRG with standard QC-DMRG across different H₂ aggregates with varying inhomogeneities. Fig 4 illustrates the rel-

TABLE I. Numerical results of BIPS-DMRG are compared with cMF and cDMRG, using the absolute ground state energy of DMRG as the reference. The results of methods other than DMRG are presented in terms of energy errors (Δ) deviating from the reference.

Systems	Reference/ E_h ^a	$\Delta(\text{HF})/\text{mE}_h$	$\Delta(\text{cMF})/\text{mE}_h$	$\Delta(\text{ASD-DMRG})/\text{mE}_h$	$\Delta(\text{BIPS-DMRG})/\text{mE}_h$
PAH/6 body ^b	-1361.147804	637.02	39.18	21.34	1.42
polyacetylene/8 body ^c	-1824.751700	1021.57	38.73	30.85	0.35
polythiophene/10 body ^d	-5441.432416	771.20	90.75	13.49	0.78
N_2 aggregate/10 body ^e	-1087.896665	4595.74	4.16	2.12	0.99
naphthalene aggregate/10 body ^f	-3825.754926	1743.13	7.99	7.99	2.95

^a QC-DMRG with $m=1000$

^b 36 electrons in 36 orbitals, $n_{\text{state}}=32$, $\tilde{m}=32$

^c 48 electrons in 48 orbitals, $n_{\text{state}}=32$, $\tilde{m}=32$

^d 60 electrons in 50 orbitals, $n_{\text{state}}=64$, $\tilde{m}=64$

^e 60 electrons in 60 orbitals, $n_{\text{state}}=16$, $\tilde{m}=16$

^f 100 electrons in 100 orbitals, $n_{\text{state}}=16$, $\tilde{m}=16$

TABLE II. State average BIPS-DMRG results for the first six energetically low-lying states of polythiophene aggregate.

State	Reference/ E_h ^a	$\Delta(\text{BIPS-DMRG})/\text{mE}_h$ ^b
$E(S_0)$	-5441.432591	2.32
$E(S_1)$	-5441.310126	5.15
$E(S_2)$	-5441.302995	4.97
$E(S_3)$	-5441.294390	4.83
$E(S_4)$	-5441.286153	6.18
$E(S_5)$	-5441.284758	6.98

^a QC-DMRG with $m=1000$

^b $n_{\text{state}}=64$; $\tilde{m}=6 \times 64=384$ (considering there are six targeted states).

ative energy errors versus the intra- and inter-molecular distances in a chain of ten H_2 molecules. With a fixed threshold for preserved local bases and a maximum of eight states, the maximum energy error occurred at the right corner of Fig 4, where the intra-molecule and inter-molecule distances are close and short ($\sim 1.5\text{\AA}$). Under such circumstance, the correlation is homogeneous and DMRG works much better than BIPS, which is designed for inhomogenous systems. Conversely, in those areas where the intra-molecular distances are dramatically smaller than the inter-molecular distances—a common situation in realistic chemical systems—the BIPS method can efficiently capture the major part of the electron correlation with errors less than 4 mE_h . This verifies again that the BIPS method is generally applicable to various molecular systems with different inhomogeneities.

CONCLUSION

In summary, we have developed an efficient method called BIPS-DMRG for describing inhomogeneous correlations, which allows us to separately address strong intra-fragment and weak inter-fragment correlations in realistic chemical systems. By employing bath orbitals

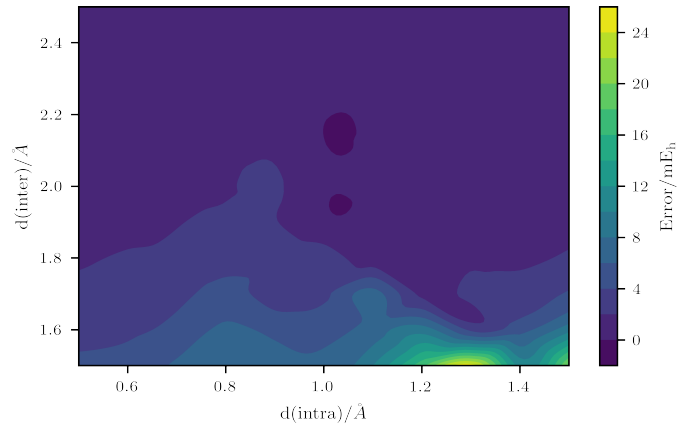


FIG. 4. Energy error surface for an aggregate of H_2 molecules relative to standard DMRG. The x-axis and y-axis respectively denote the intra-molecular and inter-molecular distances in H_2 chain (Fig 2.f).

generated from a one-shot DMET, the environmental effect is considered in the encapsulation of intra-fragment correlation. The remaining weaker, yet more homogeneous, inter-fragment interactions can be effectively described by cDMRG using a small bond dimension.

Extensive benchmarking across diverse molecular systems demonstrates that BIPS-DMRG not only surpasses conventional DMRG methods in speed for non-uniform systems, but also achieves superior compression of the local Hilbert space with diabatic states compared to isolated adiabatic eigenstates. This framework can readily accommodate non-Abelian spin-SU(2) symmetry, making the defined electronic states more physically meaningful. In the future, it will be necessary to develop more refined bath orbitals for multiple open-shell excited states. Consequently, the potential application of BIPS-DMRG to complex assemblies, particularly those involving multiple transition metal and lanthanide/actinide centers, holds great promise for advancing the understanding and

study of material properties and catalytic processes.

This work was supported by the National Natural Science Foundation of China (Nos. 22325302 and 22073045). We would like to also thank Huanchen Zhai and Junjie Yang for stimulating discussions.

* xiaoyuxie@sdu.edu.cn

† haibo.ma@sdu.edu.cn

- [1] S. R. White, Density matrix formulation for quantum renormalization groups, *Phys. Rev. Lett.* **69**, 2863 (1992).
- [2] S. R. White, Density-matrix algorithms for quantum renormalization groups, *Phys. Rev. B* **48**, 10345 (1993).
- [3] U. Schollwöck, The density-matrix renormalization group, *Rev. Mod. Phys.* **77**, 259 (2005).
- [4] U. Schollwöck, The density-matrix renormalization group in the age of matrix product states, *Ann. Phys. (N. Y.)*, 97 (2011).
- [5] T. Xiang, Density-matrix renormalization-group method in momentum space, *Phys. Rev. B* **53**, R10445 (1996).
- [6] F. Verstraete, D. Porras, and J. I. Cirac, Density Matrix Renormalization Group and Periodic Boundary Conditions: A Quantum Information Perspective, *Phys. Rev. Lett.* **93**, 227205 (2004).
- [7] S. Depenbrock, I. P. McCulloch, and U. Schollwöck, Nature of the Spin-Liquid Ground State of the $S=1/2$ Heisenberg Model on the Kagome Lattice, *Phys. Rev. Lett.* **109**, 067201 (2012).
- [8] Z. Zhu and S. R. White, Spin liquid phase of the $s=1/2$ j_1-j_2 heisenberg model on the triangular lattice, *Phys. Rev. B* **92**, 041105 (2015).
- [9] B.-X. Zheng, C.-M. Chung, P. Corboz, G. Ehlers, M.-P. Qin, R. M. Noack, H. Shi, S. R. White, S. Zhang, and G. K.-L. Chan, Stripe order in the underdoped region of the two-dimensional Hubbard model, *Science* **358**, 1155 (2017).
- [10] D. P. Arovas, E. Berg, S. A. Kivelson, and S. Raghu, The Hubbard Model, *Annu. Rev. Condens. Matter Phys.* **13**, 239 (2022).
- [11] S. R. White and R. L. Martin, Ab initio quantum chemistry using the density matrix renormalization group, *J. Chem. Phys.* **110**, 4127 (1999).
- [12] G. K.-L. Chan, A. Keselman, N. Nakatani, Z. Li, and S. R. White, Matrix product operators, matrix product states, and ab initio density matrix renormalization group algorithms, *J. Chem. Phys.* **145**, 014102 (2016).
- [13] S. Daul, I. Ciofini, C. Daul, and S. R. White, Full-CI quantum chemistry using the density matrix renormalization group, *Int. J. Quantum Chem.* **79**, 331 (2000).
- [14] H. Ma, U. Schollwöck, and Z. Shuai, *Density Matrix Renormalization Group (DMRG)-Based Approaches in Computational Chemistry* (Elsevier, 2022).
- [15] N. Chepiga and S. R. White, Comb tensor networks, *Phys. Rev. B* **99**, 235426 (2019).
- [16] C. A. Jiménez-Hoyos and G. E. Scuseria, Cluster-based mean-field and perturbative description of strongly correlated fermion systems: Application to the one- and two-dimensional Hubbard model, *Phys. Rev. B* **92**, 085101 (2015).
- [17] M. R. Hermes and L. Gagliardi, Multiconfigurational Self-Consistent Field Theory with Density Matrix Embedding: The Localized Active Space Self-Consistent Field Method, *J. Chem. Theory Comput.* **15**, 972 (2019).
- [18] H. R. Larsson, H. Zhai, K. Gunst, and G. K.-L. Chan, Matrix product states with large sites, *J. Chem. Theory Comput.* **18**, 749 (2021).
- [19] S. D. Drell, M. Weinstein, and S. Yankielowicz, Quantum field theories on a lattice: Variational methods for arbitrary coupling strengths and the ising model in a transverse magnetic field, *Physical Review D* **16**, 1769 (1977).
- [20] C. J. Morningstar and M. Weinstein, Contractor Renormalization Group Method: A New Computational Technique for Lattice Systems, *Phys. Rev. Lett.* **73**, 1873 (1994).
- [21] K. G. Wilson, The renormalization group: Critical phenomena and the kondo problem, *Rev. Mod. Phys.* **47**, 773 (1975).
- [22] K. Wang, Z. Xie, Z. Luo, and H. Ma, Low-Scaling Excited State Calculation Using the Block Interaction Product State, *J. Phys. Chem. Lett.* , 462 (2022).
- [23] Ö. Legeza, J. Röder, and B. A. Hess, Controlling the accuracy of the density-matrix renormalization-group method: The dynamical block state selection approach, *Phys. Rev. B* **67**, 125114 (2003).
- [24] G. Knizia and G. K.-L. Chan, Density Matrix Embedding: A Simple Alternative to Dynamical Mean-Field Theory, *Phys. Rev. Lett.* **109**, 186404 (2012).
- [25] S. R. White, Density matrix renormalization group algorithms with a single center site, *Phys. Rev. B* **72**, 180403 (2005).
- [26] C. Hubig, I. P. McCulloch, U. Schollwöck, and F. A. Wolf, Strictly single-site DMRG algorithm with subspace expansion, *Phys. Rev. B* **91**, 155115 (2015).
- [27] S. Lee, H. Zhai, S. Sharma, C. J. Umrigar, and G. K.-L. Chan, Externally corrected ccscd with renormalized perturbative triples (r-cccsd (t)) and the density matrix renormalization group and selected configuration interaction external sources, *J. Chem. Theory Comput.* **17**, 3414 (2021).
- [28] Q. Sun, X. Zhang, S. Banerjee, P. Bao, M. Barbry, N. S. Blunt, N. A. Bogdanov, G. H. Booth, J. Chen, Z.-H. Cui, *et al.*, Recent developments in the pyscf program package, *J. Chem. Phys.* **153** (2020).
- [29] M. R. Hermes, R. Pandharkar, and L. Gagliardi, Variational localized active space self-consistent field method, *J. Chem. Theory Comput.* **16**, 4923 (2020).
- [30] Z. Xie, Y. Song, F. Peng, J. Li, Y. Cheng, L. Zhang, Y. Ma, Y. Tian, Z. Luo, and H. Ma, Kylin 1.0: An ab-initio density matrix renormalization group quantum chemistry program, *J. Comput. Chem.* **44**, 1316 (2023).
- [31] S. M. Parker and T. Shiozaki, Communication: Active space decomposition with multiple sites: Density matrix renormalization group algorithm, *J. Chem. Phys.* **141** (2014).